FR 9102330

1979 IEEE International Conference on plasma science.
Montreal, Canada, June 4 - 6, 1979.
CEA - CONF 4802

PLASMA FOCUS RESEARCH AT THE CENTRE D'ETUDES DE LIMEIL

A. BERNARD, J.P. GARCONNET, A. JOLAS, J.P. LE BRETON,
J. de MASCUREAU and P. ROMARY

Commissariat à l'Energie Atomique, Centre d'Etudes de Limeil
B.P. n° 27, 94190 VILLENEUVE SAINT-GEORGES, FRANCE

Introduction

The purpose of the present talk is to give the most important results concerning plasma focus research at the Centre d'Etudes de Limeil. At first we will describe the structure of the current sheath during the axial propagation. Then we will speak about the singularity phase and the associate turbulent resistivity which comes before the beam phase. And we will see that plasma focus can be considered as the most powerful ion beam generator.

I - STRUCTURE OF THE CURRENT SHEATH DURING AXIAL PROPAGATION

The current distribution has been studied extensively on a 500 kA Mather type device with a solid and flat anode and a squirrel cage cathode. But the main results presented to-day were also observed on smaller and larger devices of both Mather and Filippov geometries and thus must be considered as general properties of focus experiments.

.../...

In Fig. 1 one can see the structure of the current sheath during the axial propagation phase with respect to the dense and luminous plasma sheath. The radial current density j_r is obtained directly from magnetic probe measurements as the sheath can be considered stationary. The luminous sheath profile is taken from an image converter camera with a 1 ns timing.

The important points are the following : the current sheath consists of a broad structure 1 or 2 centimeters large depending on the radial distance to the anode and on the electrode geometry. Only 10 to 20 percent of the total current flows in the dense sheath.

Most of it flows behind the dense sheath in a more tenuous plasma. Very often the current shifted to the end of the gun is a fraction only (70 - 90 %) of the total current, the larger the fraction, the most efficient is the discharge.

These results are now well known but we think that the question is : how can we explain this structure and is it possible by considering M.H.D. theory only ?

AXIAL PROPAGATION PHASE

- THE CURRENT SHEATH CONSISTS OF A BROAD STRUCTURE
- ONLY 10-20 % OF THE TOTAL CURRENT FLOWS IN THE DENSE SHEATH
- MOST OF THE CURRENT FLOWS BEHIND THE DENSE SHEATH
- THE CURRENT SHIFTED TO THE END OF THE GUN IS A FRACTION OF THE TOTAL CURRENT, THAT VARIES WITH THE QUALITY OF THE DISCHARGE

QUESTION :

- CAN M.H.D. EXPLAIN THESE PHENOMENA ?

TABLE I

.../...

II - SINGULARITY PHASE

The collapse phase too has been studied by magnetic probe techniques and also by ruby laser scattering which is a nonperturbing method to derive information on macroscopic and microscopic plasma parameters. Measurements are performed in a 27 kJ - 500 kA Mather type device. When the plasma sheath begins the radial implosion, the current density increases rapidly due to geometrical effect and one observes singularities on the electrical signals that is current derivative and voltage.

In Fig. 2 we see typical probe signals relative to the radial collapse for 3 radial positions of the probe. It is very clear that current is still flowing at r = 20 since $\frac{dB}{dt} > 0$ when $\frac{dI}{dt}$ is minimum (t_{min}). Thus electrical singularities must be explained in terms of an anomalous ohmic resistance. Taking into account absolute probe calibration one can estimate that the average conductivity reaches a minimum in the range of 10^{12} to 2×10^{11} sec^{-1} that is to say 10^{-3} to 10^{-4} Spitzer's value assuming an electron temperature of 50 eV. But this estimate would not change very much with temperature. From electrical measurements outside the plasma gun we derive the maximum plasma resistance $R = (V - L\dot{I})\, I^{-1}$ which varies little for all our machines when optimized and is in the range of 0.2 - 0.4 Ω. It is interesting to note, however, that R varies with filling pressure: for instance we have on average 70 mΩ at 8 Torr and 250 mΩ at 1 Torr for the 500 kA machine. In order to study the microscopic instabilities responsible for this anomalous conductivity we have developed a ruby laser scattering experiment. A schematic outline of the arrangement appears in Fig. 3. With respect to the laser beam scattered light is observed at 120°, 90°, 60° and in the forward direction at 7°. These various observation angles correspond to different wavenumbers and allow us to measure the wavenumber spectrum. In the forward observation (7°) we are able to measure the angular distribution (angle θ) of scattered light (with the same wavenumber). This system thus gives in a single shot the wavenumber spectrum $n_e\, S(k)$ and the angular distribution $n_e\, S_{k=7°}(\theta)$ of electron density fluctuations after a Rayleigh scattering experiment for calibration

S is the spectral density function

θ is the angle between the scattering vector k

and the z axis of the electrodes ; n_e is the electron density.

.../...

Movable electrodes give the possibility of a spatial study of the plasma. The results presented to-day refer to the region located at 10 mm from the anode and 12.5 mm from the z axis (the anode diameter is 50 mm). Filling pressure is 8 Torr of hydrogen . At this pressure the maximum value of the anomalous resistance is in the range of 70 mΩ .

The scattered signals are analysed with a 2 ns time resolution and carefully readjusted with respect to the dense plasma sheath position. We obtain scattered signals when the dense and luminous layer crosses the observed region, but also before the layer reaches this region and after it has passed.

The scattered signals are different in these three situations and we interpret the scattering obtained before and after passage of the dense layer as turbulent scattering, while the layer itself gives signals compatible with a thermalized plasma.

An example of the results obtained when scattering is due to the dense sheath is shown in Fig. 4.

We see that the forward scattering is isotropic and that n_e S (k) is flat in the k range considered.

According to Salpeter theory for thermalized plasma, this is possible if signals are due to the ion component and if the parameter $\alpha = \frac{1}{k \lambda_D}$ is greater than 2 for all the considered k vectors. Assuming $\frac{1}{k \lambda_D} = 2$ for the 120° scattering we obtain the following parameters :

$$S = 0.5 \quad \text{(ion component)}$$
$$n_e = 1.4 \times 10^{18} \text{ cm}^{-3}$$
$$\lambda_D = 3.2 \times 10^{-6} \text{ cm}$$
$$T_e \lesssim 30 \text{ eV}$$

if one assumes equilibrium between ion and electron temperatures.

.../...

When the dense layer is not in the field of observation at the instant of the laser pulse, we obtain scattered signals which are measurable only in the 7° channel. In the 60°, 90° and 120° channels the signals are lower than or equal to the detection threshold, which is 5×10^{16} cm^{-3}, when the plasma own light is taken into account. The amplitude of the signals scattered at 7° and the anisotropy as a function of orientation of k result in S(k) taking values much higher than unity, i.e. a suprathermal level of density fluctuations is established in the tenuous region of the plasma with predominant directions of propagation. The signals are detectable at r = 12.5 mm as soon as the dense layer attains r = 20 mm. Until the arrival of the layer the S_k (θ) spectrum retains the same bell shape of curve (Fig. 5 a), the maximum value of n_e S(k) varies from 3×10^{17} to 10^{18} cm^{-3} depending on the particular shot. It will be noted that the 0° and 90° directions correspond to minima.

The signals are measurable at this point (r = 12.5, z = 10), while the layer gathers on the discharge axis, forming a filament, and even after the latter's dislocation. The shape of the S_k (θ) spectrum differs from that in the preceding cases, here exhibiting a maximum for the 0° or 22° 30' direction, while the 90° direction remains the minimum (Fig. 5 b). The maximum value of n_e S(k) varies between 5×10^{17} and 5×10^{18} cm^{-3}.

These results therefore are consistent with magnetic probe measurements which showed that the electric current circulated mostly outside the dense plasma layer.

Clearly in order to identify microscopic instabilities, detailed investigation and frequency spectra are required but we can point out the following : Table II.

.../...

SINGULARITY PHASE

- THE COLLAPSE IS CORRELATED WITH A STRONG ANOMALOUS RESISTANCE

- SEVERAL RADIAL REGIONS MUST BE CONSIDERED

  NEARLY THERMAL HIGH DENSITY SHEATH

  HIGHLY TURBULENT LOW DENSITY ZONES

- ELECTRICAL CURRENT CIRCULATES MOSTLY OUTSIDE THE DENSE PLASMA SHEATH

- NO HARD X RAYS OR NEUTRONS ARE OBSERVED DURING THIS PHASE

Table II

.../...

III - BEAM PHASE

When the resistance reaches its maximum the electrical current is suddenly carried by intense beams of electrons and ions. In other words the resistive regime is sharply interrupted by a beam regime.

Electron beams

Several laboratories have shown that electron beams generated in a plasma focus are very intense. Briefly we would like to report the properties of electron beams generated by the 340 kJ facility of Limeil.

Taking into account the yield and spectrum of the X radiation, one can estimate :

340 kJ - 40 kV LIMEIL FACILITY
X-RADIATION
150 JOULES ABOVE 5 keV MAXIMUM AT 60 kV TIME DURATION 35 NSEC
ELECTRON BEAM
$200 < E_e < 300$ keV
$10 < W_e < 15$ kJ
$0.4 \times 10^{12} < P_e < 0.8 \times 10^{12}$ W

Table III

Ion beams

Now we would like to give the last results concerning ion beams. Focus experiments are known to have the highest neutron yield of laboratory plasma;we will see that for optimized conditions, plasma focus can be considered as the most powerful ion beam generator .

.../...

It has been shown that more than 85 % of the neutrons are created by high energy deuterons accelerated in the plasma in front of the anode and bombarding the surrounding plasma and gas.

A series of experiments has been conducted with various metal screens and diaphragms placed in front of the anode parallel to the anode end plane and by measuring the anisotropy of the neutron emission (Fig. 6). The plasma is created by the 27 kJ-40 kV device. The following is shown : the yield, the anisotropy and the time duration of the neutron emission decrease when a screen is placed a few centimeters in front of the anode.

When a small diaphragm (10 mm diam.) is placed at 10 mm from the anode the anisotropy becomes maximum. We have obtained anisotropy greater than 3 in these conditions.

This means that the high energy component ($E_i \geq 300$ keV) is strongly forward directed while the lower energy component which generates the major part of the neutrons is rather an open conical beam. This later component is stopped by the diaphragm.

In order to know whether these ion beams can be delivered on targets we have placed a deuterated polyethylene plate in front of the anode(Fig. 6). This experiment as been done on both 27 kJ and 340 kJ facilities. Results are shown in Fig. 7 for the 340 kJ case with a 3 cm diam. target. One can see clearly that the waveform of the dN/dt is different when the CD_2 target is used, that is the pulse duration is shorter and the maximum higher. This is due to the fact that the deuteron in a CD_2 target loses his energy on a very short range. Thus the pulse width of the dN/dt is the beam emission time. The hatched area represents 10^{11} neutrons and corresponds to the minimum number of neutrons that come from the target. Taking into account the anisotropy of the neutron emission one gets an average energy of 300 keV for the deuterons. One then calculates an ion current of 1 MA during 40 ns corresponding to 12 kJ and a power of 0.3×10^{12} W.

Table IV shows the ion beam characteristics delivered on a CD_2 target for two different facilities.

.../...

TABLE IV

Ion beams delivered on a 3 cm diam. CD_2 target

	FACILITIES	
	27 kJ 0.53 MA	340 kJ 2.5.MA
neutron anisotropy	2	3
deuteron energy E_i	100 keV	300 keV
deuteron current I_i	0.125 MA	1 MA
total energy W_i	0.5 J	12 kJ
power P_i	1.25×10^{10} W	0.3×10^{12} W

As the number of experiments with target has been relatively limited compared to the data obtained with ordinary gas filling it would not be appropriate at this stage to draw quantitative scaling laws from these two columns . It is clear however that there is a strong increase.

.../...

Pinhole imaging of fast ions

In order to observe the spatial emission of the fast ions we have developed pinhole cameras with solid track detectors.

We used several cameras side-on and end-on which are sketched in Fig. 8.

The magnification is 0.1 and pinholes of 50 or 100 μm diam. have been used. Kodak LR 115 type I cellulose nitrate film is used to record the fast ions. This film is insensitive to light, X rays, electrons and ions below 10 keV/nucleon. After exposure, tracks are revealed by a NaOH solution. Our preliminary results are the following : the observed tracks are not identical and correspond to an ion distribution ranging from 10 up to 250 keV. Few tracks make a hole in the 6 μm of nitrate and the range of a 250 keV proton in nitrate is 8 μm.

In the side-on cameras the number of tracks varies from shot to shot very much, even for shots giving the same resistance and the same neutron yield. This is due to a strong anisotropy of the deuteron beams emitted at 90°. We observe a greater number of tracks at 1 Torr than at 3 Torr where neutron yield is maximum.

Very often the side-on and end-on images look like a cloud of 1 to 6 cm^3 in front of the anode. It is interesting to note that a clump of very particular tracks appears in a small area (a few mm^3) located 1 - 2 cm off the anode. These tracks (10 - 100 side-on, 100 - 1000 end-on) are different from the others because they make a hole in the film and thus correspond to high energy particles.

In Fig. 9-10 we see reproductions of end-on images.

Thus these results show that even for a high pressure regime we observe anisotropy for deuteron beams emitted at 90° from axis.

.../...

CONCLUSION

It has been shown that very powerful beams of electrons and light ions can be generated by current-driven turbulence in a plasma focus.

Ion currents in excess of 1 MA can already be delivered on targets with a relatively modest capacitor banc of 340 kJ at 40 kV.

Extrapolation to higher current appears possible without fundamental difficulty and will lead to higher ion energy required for inertial confinement studies.

Structure of the current sheath during the axial propagation phase

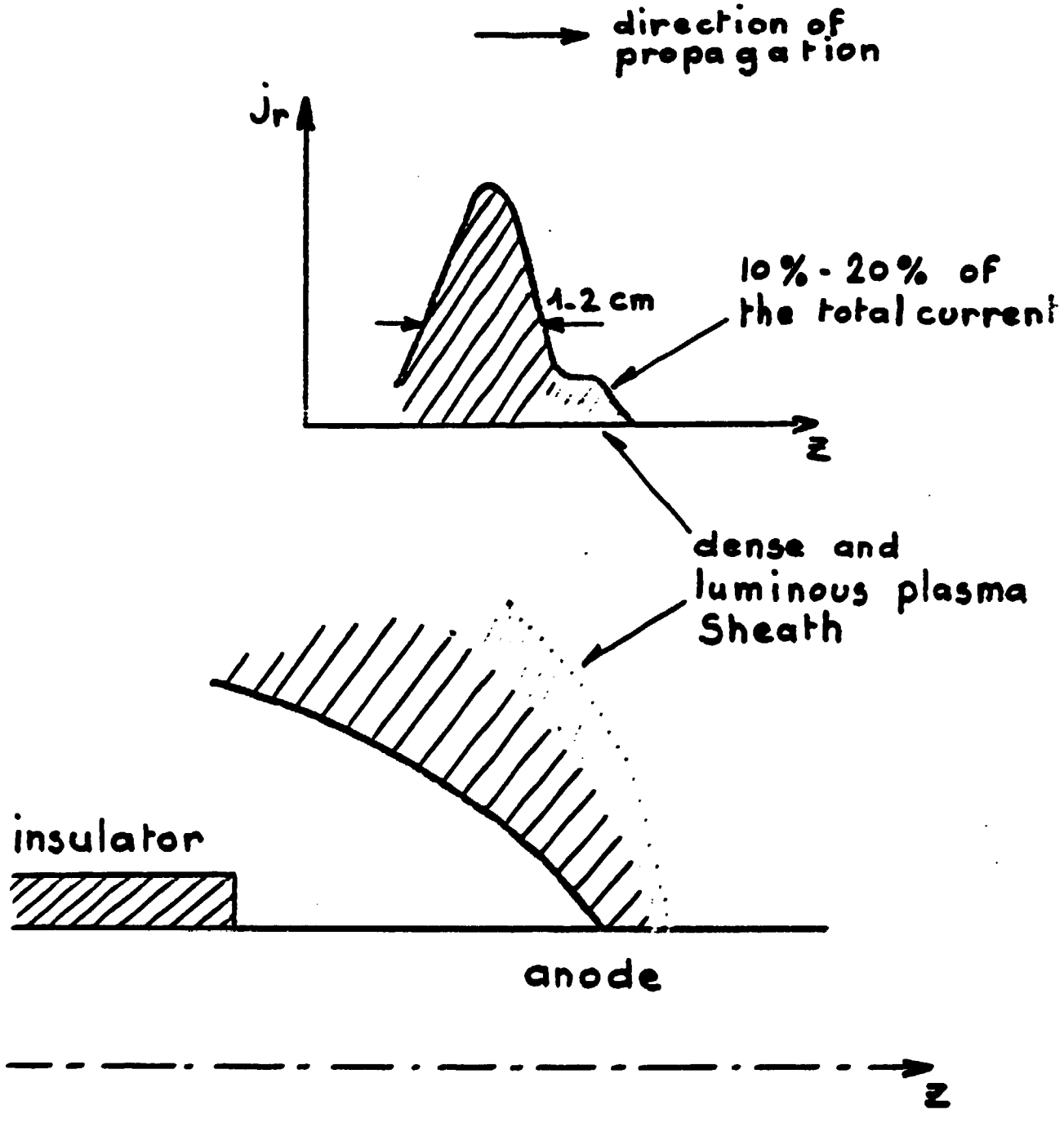

Fig.1

Fig : 2

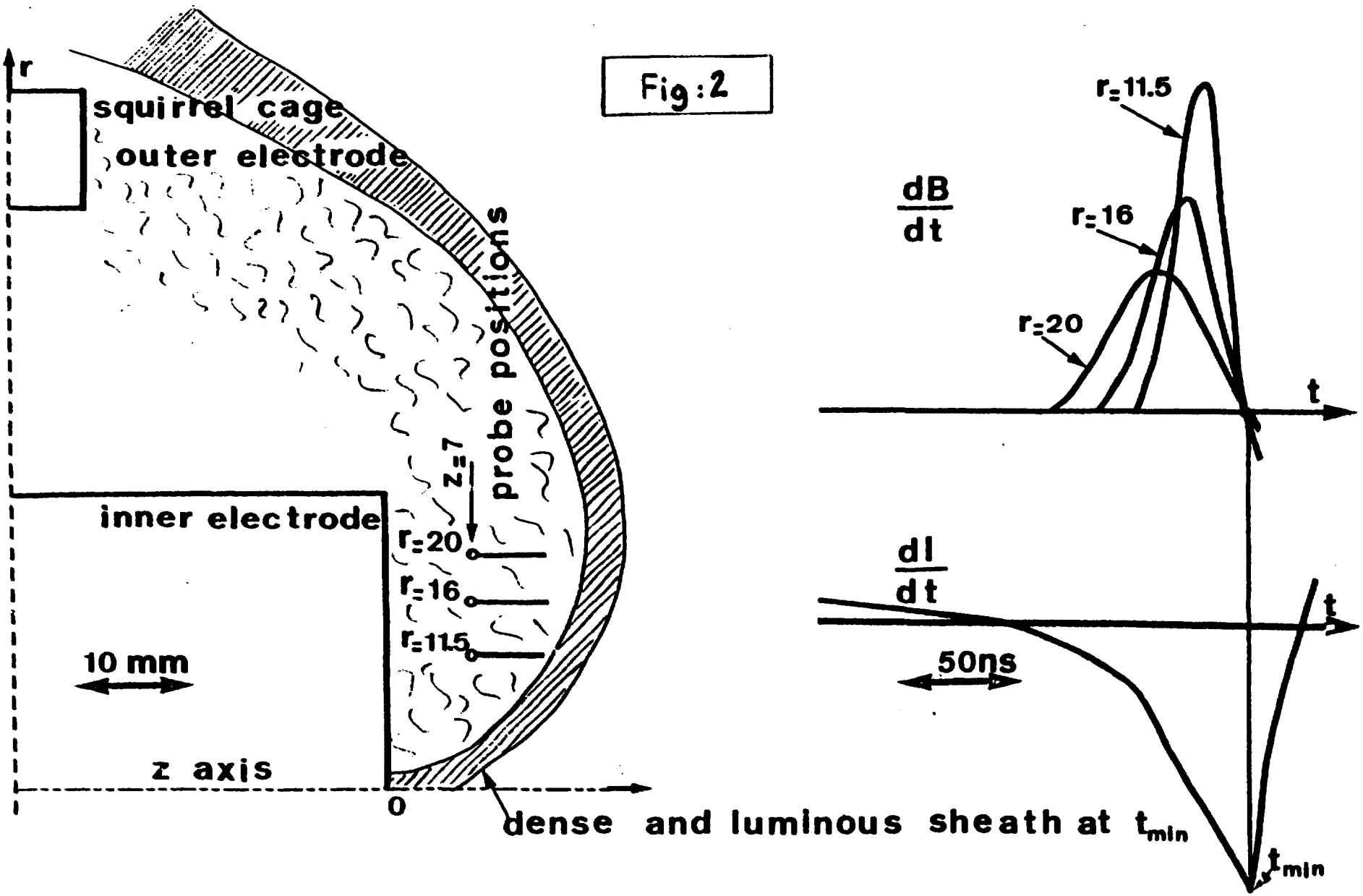
r
squirrel cage
outer electrode
probe positions
z=7
inner electrode
r=20
r=16
r=11.5
10 mm
z axis
0
dense and luminous sheath at t_{min}
dB/dt
r=11.5
r=16
r=20
t
dI/dt
t
50ns
t_{min}

Fig: 3

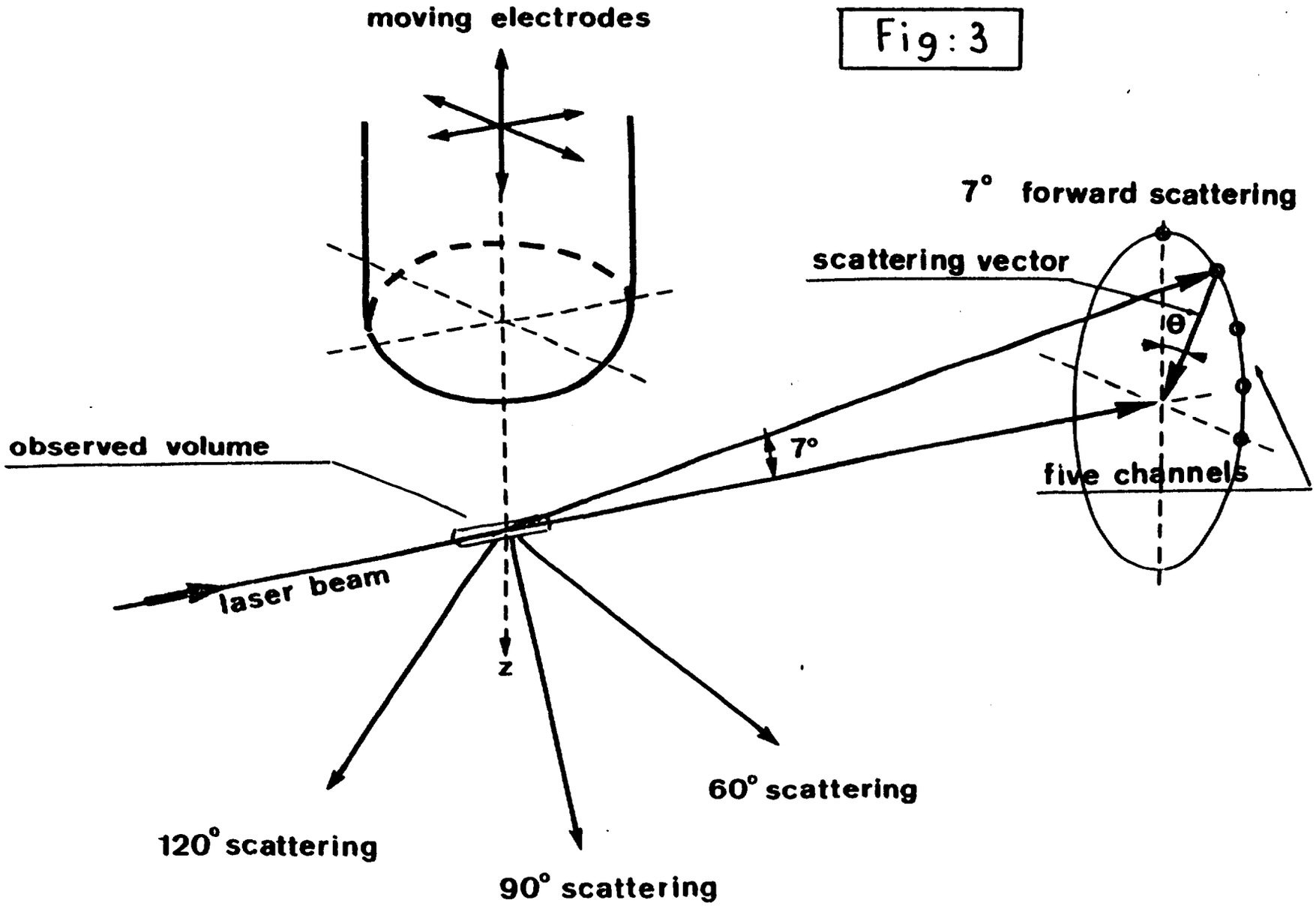
moving electrodes
7° forward scattering
scattering vector
θ
observed volume
7°
five channels
laser beam
z
60° scattering
120° scattering
90° scattering

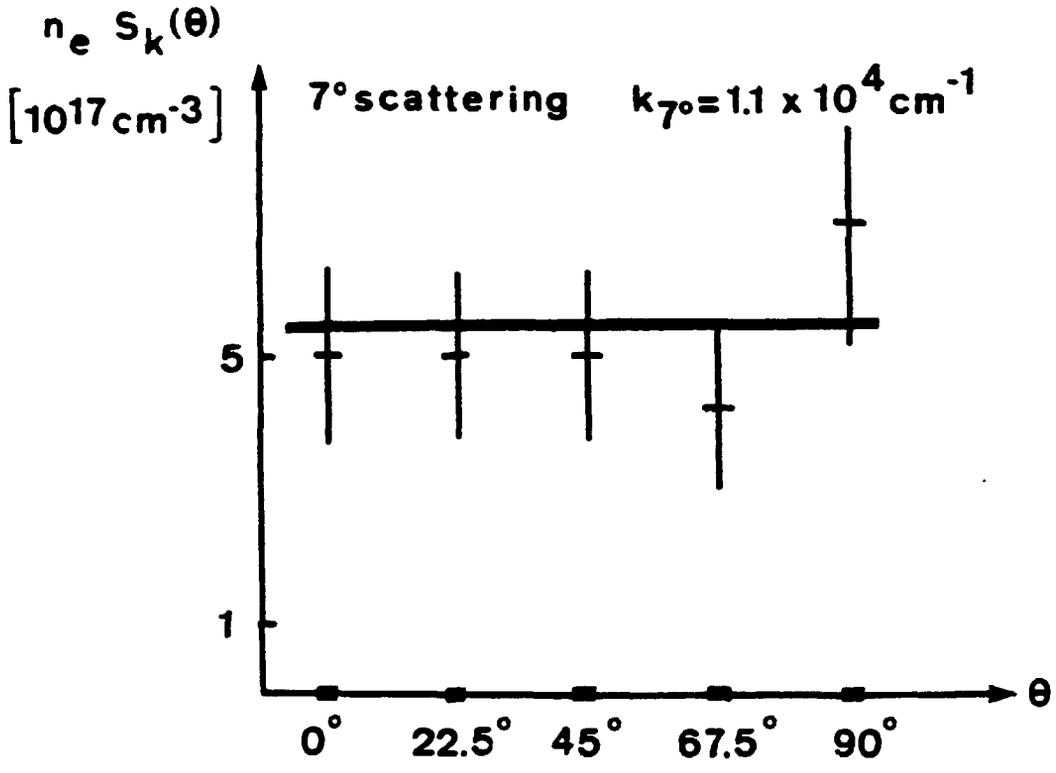
$n_e S_k(\theta)$
$[10^{17} cm^{-3}]$
7° scattering
$k_{7°} = 1.1 \times 10^4 cm^{-1}$
5
1
θ
0°
22.5°
45°
67.5°
90°

Fig: 4 (a)

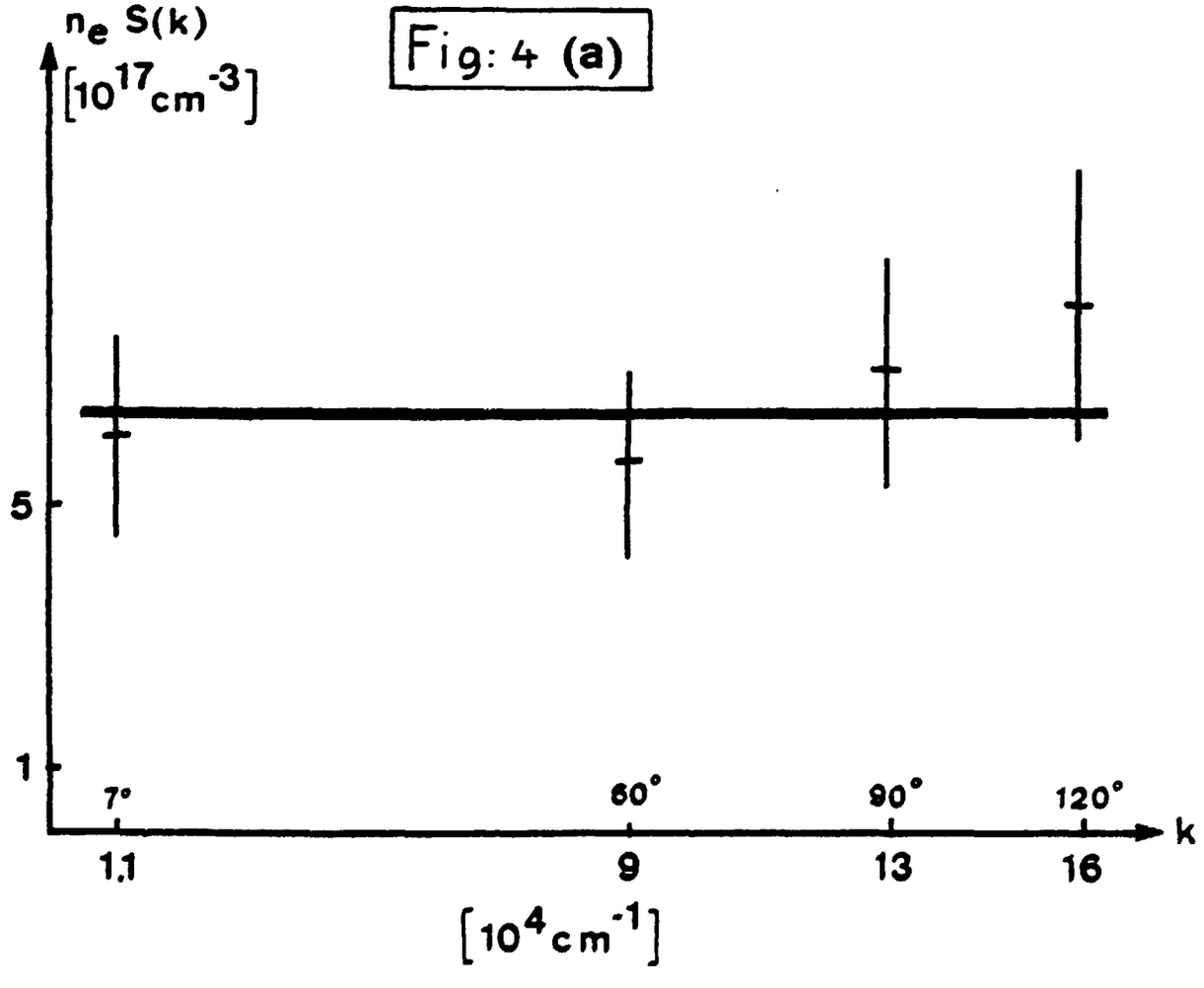
$n_e S(k)$
$[10^{17} cm^{-3}]$
5
1
7°
60°
90°
120°
k
1.1
9
13
16
$[10^4 cm^{-1}]$

Fig: 4 (b)

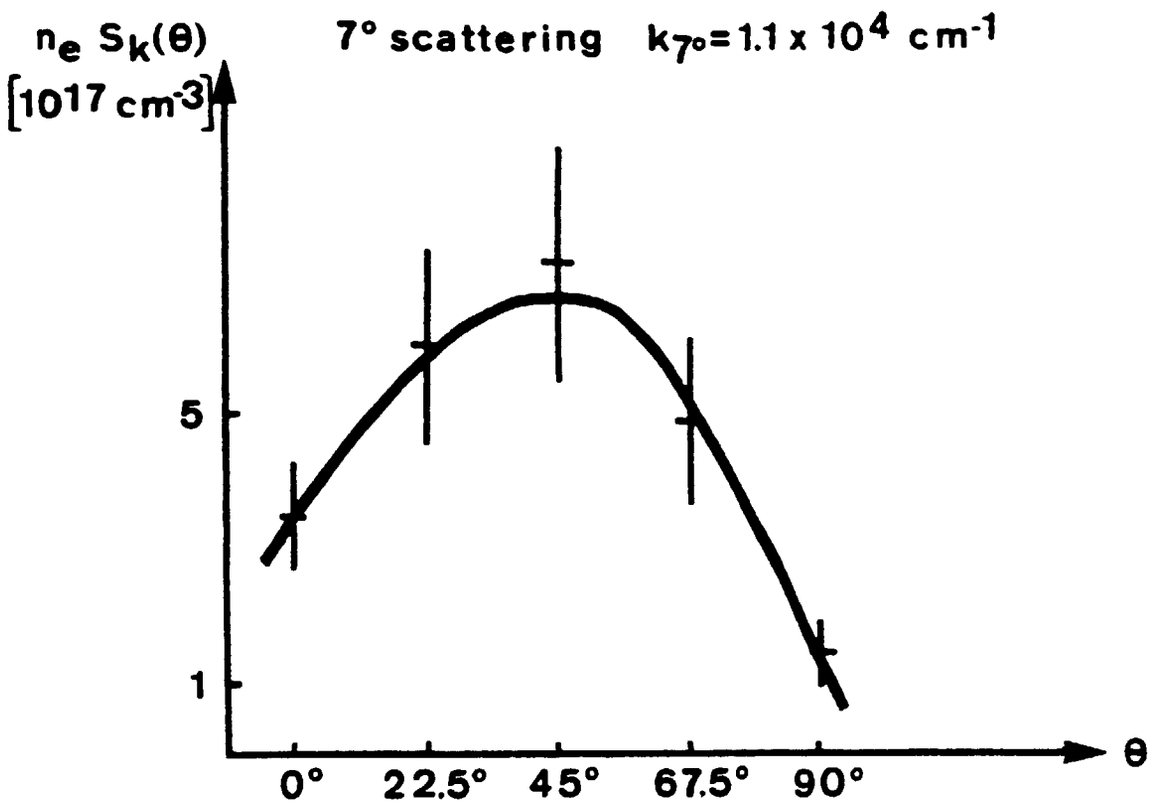
$n_e S_k(\theta)$
$[10^{17} cm^{-3}]$
7° scattering $k_{7°} = 1.1 \times 10^4 cm^{-1}$
5
1
0°
22.5°
45°
67.5°
90°
θ

Fig: 5 (a)

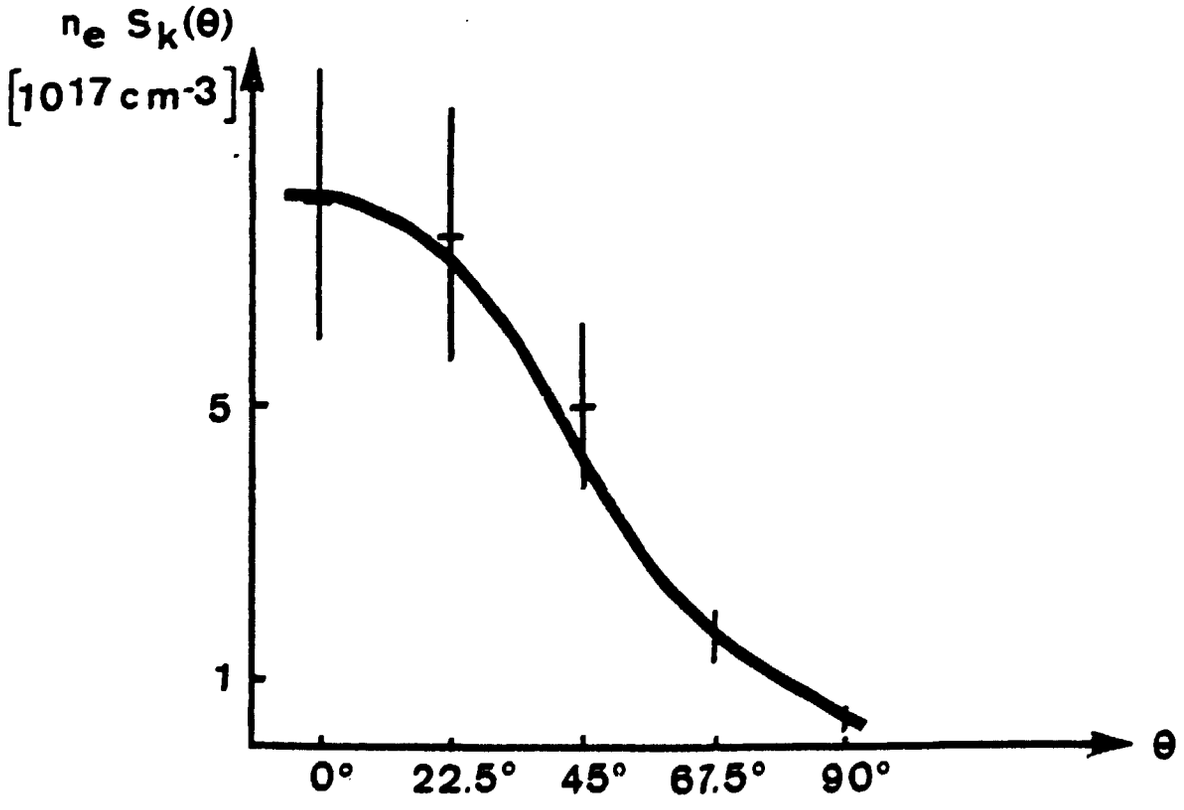
$n_e S_k(\theta)$
$[10^{17} cm^{-3}]$
5
1
0°
22.5°
45°
67.5°
90°
θ

Fig: 5(b)

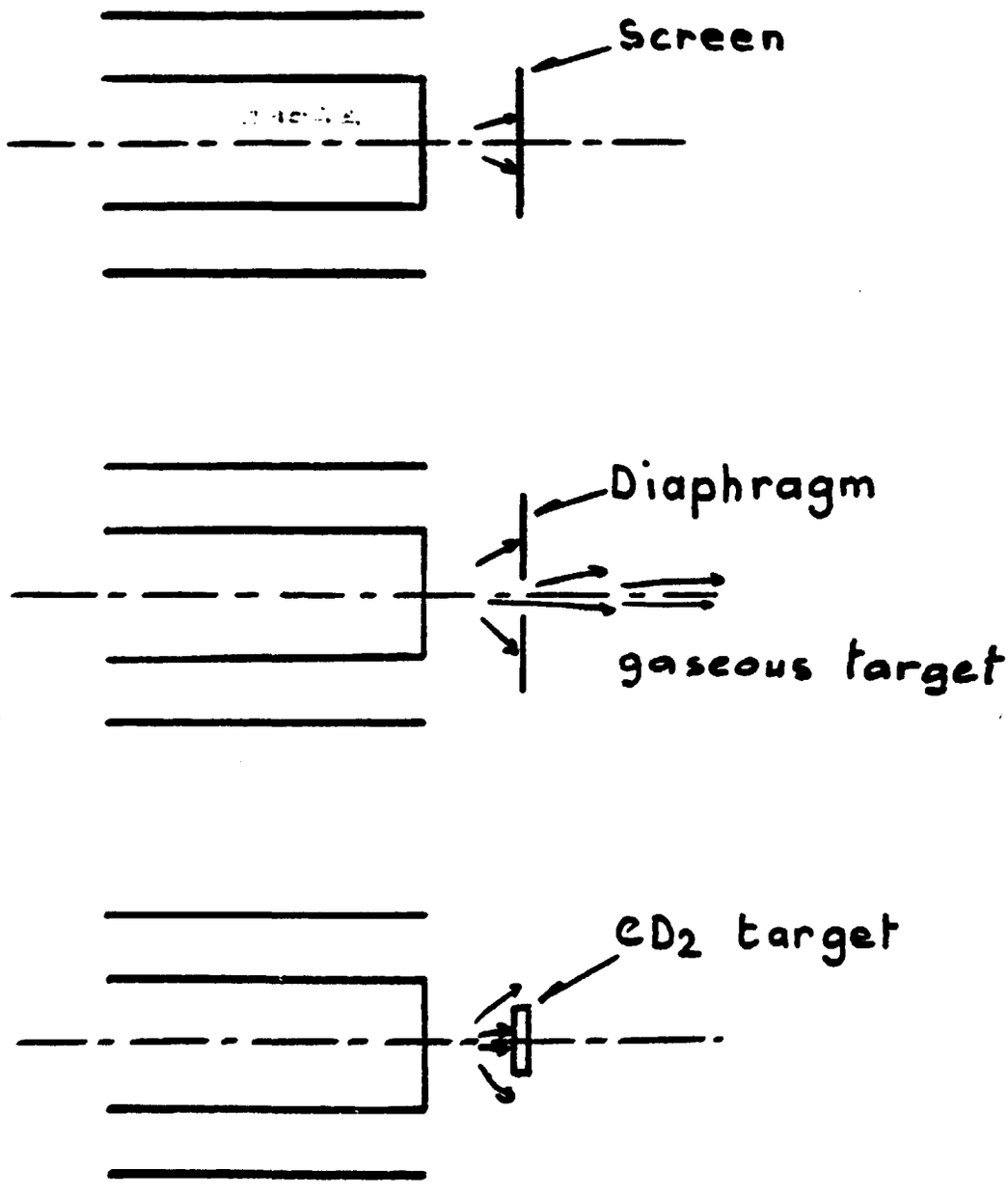

Fig: 6

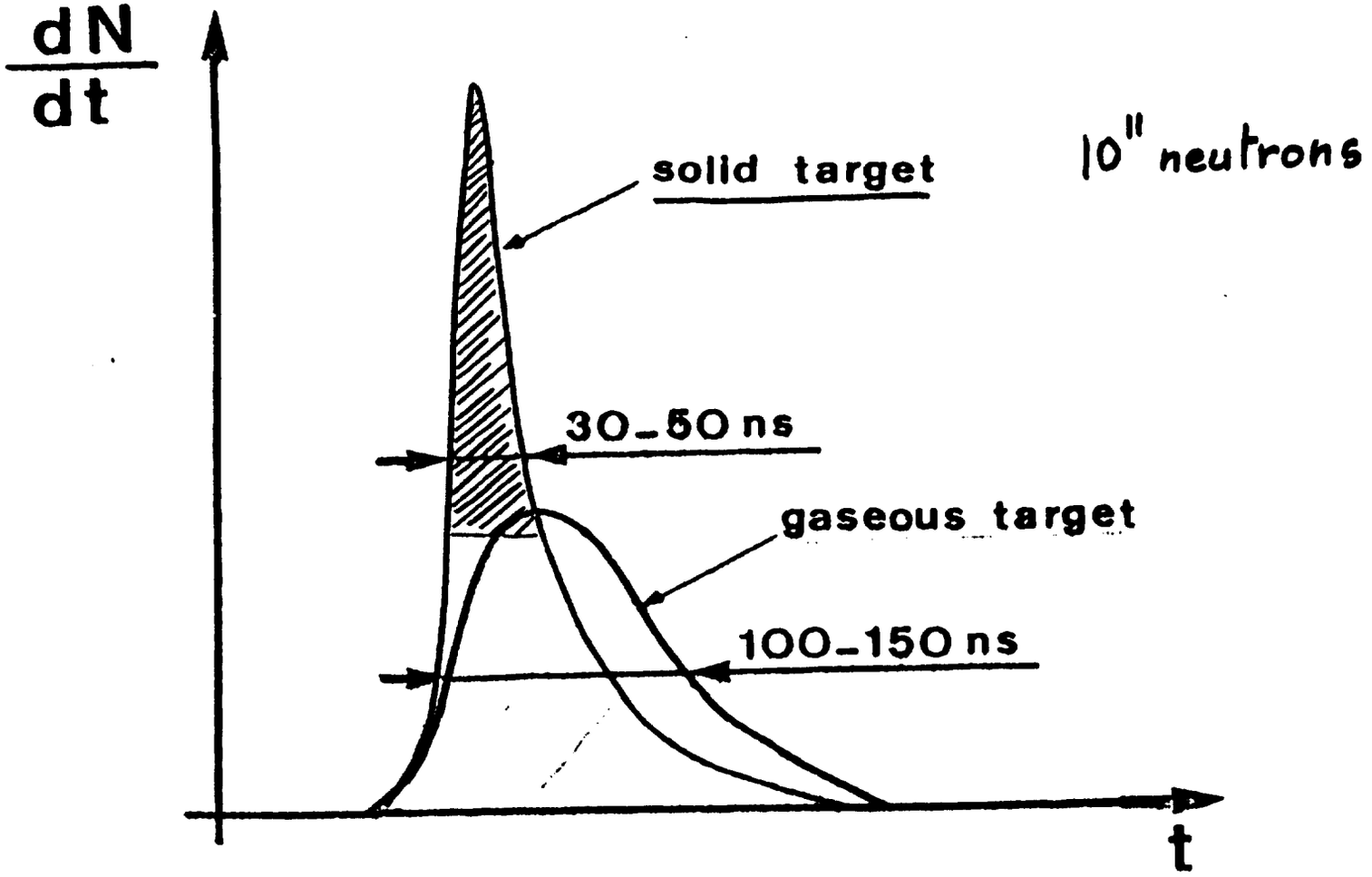
dN/dt
solid target
10^11 neutrons
30-50 ns
gaseous target
100-150 ns
t

Fig:7

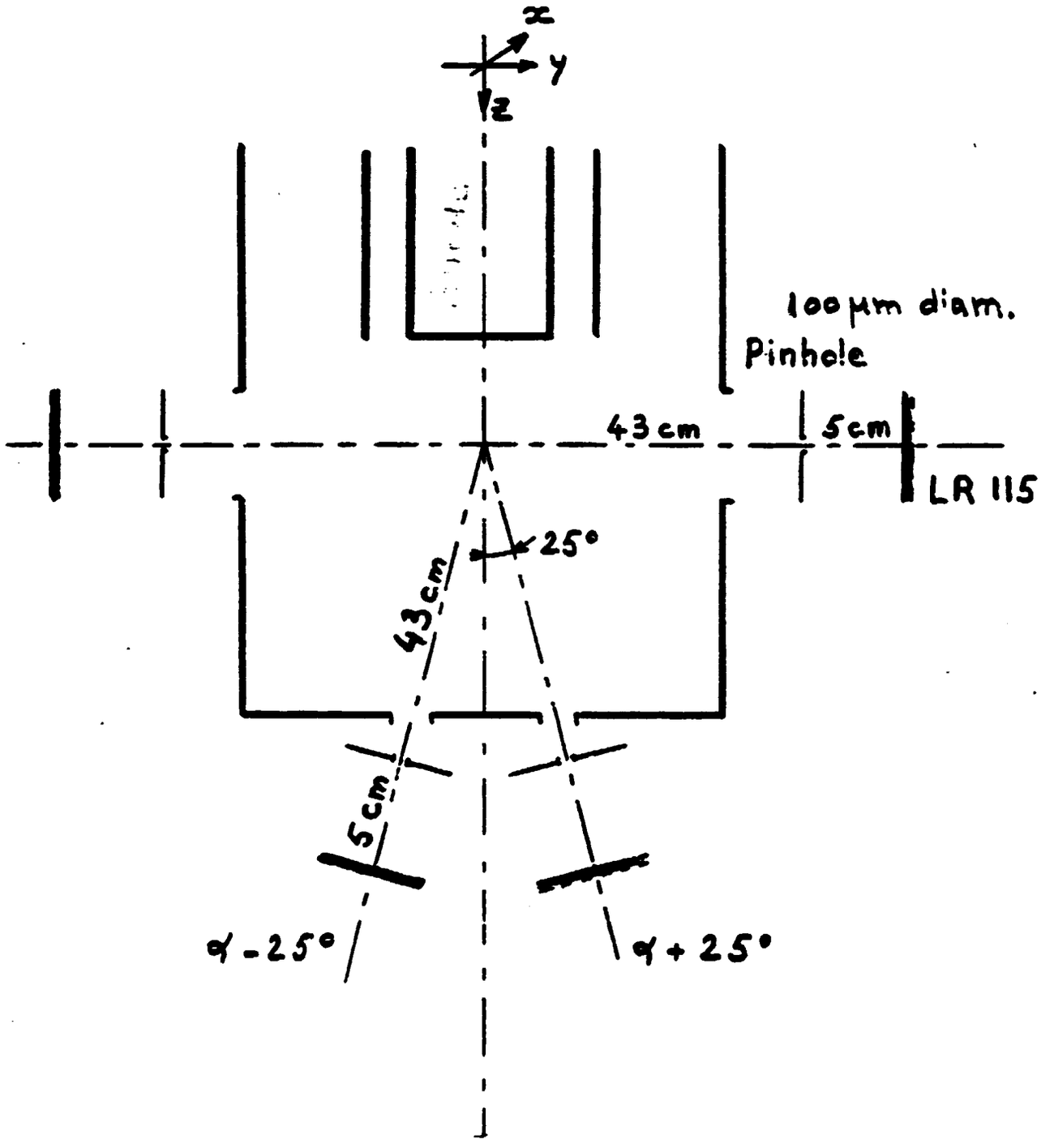

Finhole imaging of fast ions

Fig: 8

Fig:9

Fig : 10